EurJIC
European Journal of Inorganic Chemistry

Research Article
doi.org/10.1002/ejic.202300152

Chemistry Europe
European Chemical Societies Publishing

www.eurjic.org

Special Collection

Surface-Modified Carbon Materials for CO_2 Electroreduction

Francesco Mattarozzi[+],[a] Marisol Tapia Rosales[+],[a] Rim C. J. van de Poll,[b] Emiel J. M. Hensen,[b] Peter Ngene,[a] and Petra E. de Jongh*[a]

The electrochemical reduction of CO_2 to produce sustainable fuels and chemicals has attracted great attention in recent years. It is shown that surface-modified carbons catalyze the CO_2RR. This study reports a strategy to modify the surface of commercially available carbon materials by adding oxygen and nitrogen surface groups without modifying its graphitic structure. Clear differences in CO_2RR activity, selectivity and the turnover frequency between the surface-modified carbons were observed, and these differences were ascribed to the nature of the surface groups chemistry and the point of zero charge (PZC). The results show that nitrogen-containing surface groups are highly selective towards the formation of CO from the electroreduction of CO_2 in comparison with the oxygen-containing surface groups, and the carbon without surface groups. This demonstrates that the selectivity of carbon for CO_2RR can be rationally tuned by simply altering the surface chemistry via surface functionalization.

Introduction

Anthropogenic CO_2 emissions are a main cause of climate change. Hence, the capture and electrochemical conversion of CO_2 (CO_2RR – CO_2 reduction reaction) to fuels or chemicals is an attractive strategy to achieve circularity, at least when renewable electricity is the energy source. However, the efficient electrochemical conversion of CO_2 is still challenging, due to its poor solubility in water (33 mM) and the competing reduction of protons to hydrogen in aqueous electrolytes. Therefore, efficient electrocatalysts are essential to achieve large currents and selectivity in CO_2RR.[1,2]

Carbon-based materials gained much interest as electrocatalysts, due to their low cost and abundance, their high electrical conductivity, and the possibility to tune their textural properties and surface chemistry. The main drawback for carbon as an electrode material for electrochemical CO_2 reduction is its low selectivity towards CO_2 over H^+ reduction, hence forming mostly hydrogen in aqueous solution. Wu et al.[3] reported a very low activity (< 5% faradaic efficiency) towards CO_2 electrocatalytic reduction of pristine carbon nanotubes, even at −1.2 V vs RHE. The low activity is due to low concentration of the surface defects (active sites) compared to doped-carbon materials.[4] DFT calculations gave a large energy barrier (3.0 eV) to activate CO_2 on a defect-free graphitic structure, considering the first electron transfer to adsorb CO_2 the rate determining step of the reaction.[5] Therefore, several approaches to modify carbon-based electrocatalysts and generate surface defects have been developed to enhance the catalytic activity towards the CO_2RR.

Heteroatoms and structural defects have been introduced in the graphitic carbon matrix to improve the catalytic performance.[6–12] It was shown that by synthesizing carbon monolith with high nitrogen content (0.28 wt%), it was possible to increase the CO_2 adsorption of activated carbon 1.5-times (mmol CO_2 adsorbed per gram of material) at 25 °C and 1 bar.[13] In electrocatalysis, different research groups reported that nitrogen-doped carbon materials enhanced selectivity towards the CO_2RR.[14–18] This has been ascribed to the strong adsorption of the electrophilic CO_2 carbon atom on the electron-rich nitrogen atoms at the carbon electrode surface.[19] This leads to a lower activation energy to generate the first reaction intermediate $*COO^-$ and hence a faster first electron transfer to CO_2, compared to pure graphitic carbons. Hence, high concentration of nitrogen atoms in the carbon structure or nitrogen-containing surface groups are favorable.

Two main strategies are commonly adopted for the synthesis of N-doped carbon electrocatalysts: top-down approaches (hydrothermal, mechanical exfoliation, plasma treatment and arc-discharge method) and bottom-up approaches (chemical vapor deposition, solvothermal method and free-radical polymerization).[20,21] The former generally use commercially available carbons as starting materials, while the latter use nitrogen rich organic compounds as precursors, which allow to tune the nitrogen content in the graphene layers.[21] For instance, the synthesis of N-doped graphene quantum dots via a multi-step procedure, involving the oxidation of commercially available graphite powder, graphene oxide exfoliation and

[a] F. Mattarozzi,[+] M. Tapia Rosales,[+] Dr. P. Ngene, Prof. Dr. P. E. de Jongh
Materials Chemistry and Catalysis, Debye Institute for Nanomaterials Science, Utrecht University, Universiteitsweg 99, 3584 CG Utrecht (The Netherlands)
E-mail: p.e.dejongh@uu.nl
Homepage: http://www.uu.nl/staff/PEdeJongh/Profile

[b] R. C. J. van de Poll, Prof. Dr. E. J. M. Hensen
Laboratory of Inorganic Materials and Catalysis, Department of Chemical Engineering and Chemistry, Eindhoven University of Technology, 5600 MB Eindhoven (The Netherlands)

[+] These authors contributed equally to this work.

Supporting information for this article is available on the WWW under https://doi.org/10.1002/ejic.202300152

Special Collection Part of a joint Special Collection with ChemCatChem and EurJOC on the Netherlands Institute for Catalysis Research.

Research Article
doi.org/10.1002/ejic.202300152

functionalization with dimethylformamide, represents an example of top-down approach.[20] This carbon-based electrocatalyst possessed 6 at% N atoms and produced C_2 (31% FE) and C_2 oxygenated products (26% FE) at −0.75 V vs RHE. Alternatively, imidazole-type groups were introduced on the surface of oxidized graphitic carbon materials by exploiting the high reactivity of thionyl chloride to generate an acid chloride intermediate, achieving a 35% selectivity towards ethanol at $-1.0\ mA\,cm^{-2}$.[22] Other groups focused their attention on synthesis routes that allow good control over the catalyst morphology and nitrogen content. For instance, it has been shown that starting from different molar ratios of L-cysteine and melamine precursors, it is not only possible to control the total nitrogen content in the pyrolyzed carbon matrix in the range between 3.9 at% and 5.8 at%, but also to tune the pyridinic to pyrrolic groups ratio from 1.2 to 0.7. A good correlation between higher pyridine atomic percentage and CO productivity was found, as the CO partial current density linearly increase with the pyridinic nitrogen content.[23]

Besides nitrogen-modified carbon, some researchers have also looked at the effect of oxygen-containing functional groups on the CO_2RR. Typically, either an acidic treatment at high temperatures or oxygen plasma treatment are used to introduce oxygen-containing groups on the surface.[7,24] Yang *et al.* recently showed a linear increase in the formate selectivity with increasing number of carboxylic groups, and proposed a synergistic effect between carboxylic groups and other oxygen-containing moieties (hydroxy, epoxide, and carbonyl) that steered the selectivity towards formate production (80% FE).[24]

As laborious multi-step methods were previously investigated, herein we developed a simple and scalable procedure to modify the surface of commercially available carbon materials, to specifically probe the effects of the surface properties of carbon on the electrocatalytic activity and selectivity towards the CO_2RR. Oxygen-containing surface groups were introduced via a single-step liquid phase oxidation procedure. Nitrogen-containing groups were anchored on the carbon surface through gas-phase amination after the oxidation procedure, while carbon with negligible surface groups was obtained by removing surface groups through a gas-phase reduction in hydrogen. The careful characterization allowed us for the first time to quantify the intrinsic activity (turnover frequency) of specific CO_2RR active sites, proving the remarkable performance of pyridine-like surface groups for CO production.

Results and Discussion

Tuning the surface properties of graphitic carbon

We modified pristine commercial carbon graphene nanoplatelets (GNP-P) by three different methods. The carbon was first oxidized in concentrated nitric acid (GNP-O) and then converted into either nitrogen-modified carbon (GNP-N) via gas phase amination or H_2-reduced carbon (GNP-H). These treatments introduced different functional groups on the carbon surface which allowed to study the effect of these groups on the electrocatalytic performance. The physical properties of the surface-modified carbons are summarized in Table 1.

GNP-P carbon had a BET surface area of $490\ m^2\,g^{-1}$, however, upon the oxidation a 10.8% surface area loss was observed. When the GNP-O was thermally reduced (GNP-H) or aminated (GNP-N) the surface area decreased further by 7.5% and 22.6%, respectively. The reduction of the surface area for GNP-O can be attributed to limited textural damage during the oxidative treatment,[25–27] while the high temperatures, used during the reduction and amination of the carbon surface (400 °C and 600 °C, respectively), caused a further reduction in surface area.[28] During the catalytic tests, the current density results were normalized by carbon surface area, while only the samples with a similar pore volume were tested (GNP-O, GNP-N and GNP-H).

The PZC, obtained by acid-base titration, of the surface-modified carbons (Figure 1) defines the average acid-base properties of the carbon surface and decreased in the following order: GNP-N > GNP-H > GNP-P > GNP-O. The as-received graphitic carbon (GNP-P) was acidic with a PZC value of 3.7. The acidity of GNP-P originates from native oxygen-containing functional groups.[26,29,30] The GNP-O was more acidic than GNP-P, with a PZC value of 2.3 due to the strong acidic groups introduced by the HNO_3 treatment. The surface of GNP-H was neutral with a PZC value of 7.3, possibly due to the disappearance of the acidic groups when heated in a reducing atmosphere.[31,32] The GNP-N was basic with a PZC value of 9.1, resulting from the introduction of basic groups upon amination treatment. The origin of the surface basicity of GNP-N is ascribed to the presence of N-containing groups, as when heated in O_2 atmosphere, nearly two times more NO/NO_2 was

Table 1. Surface area and porosity of the modified carbons.

Sample	BET surface area [$m^2\ g^{-1}$]	Total pore volume [$mL\ g^{-1}$]
GNP-P	490	0.84
GNP-O	437	0.78
GNP-N	338	0.73
GNP-H	404	0.76

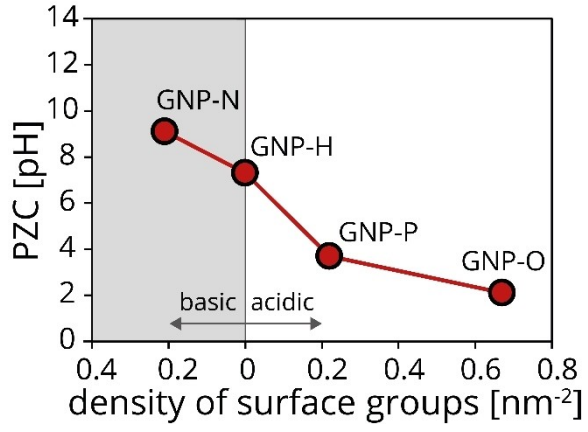

Figure 1. Point of zero charge as a function of the density of surface groups of the GNP-P, GNP-O, GNP-N and GNP-H electrocatalysts.

Research Article
doi.org/10.1002/ejic.202300152

released than for GNP-H and GNP-O (Figure S1).[28,33] These results show that the PZC of GNP-P surface can be tuned within a broad pH range from 2.3 to 9.1.

The change in PZC correlates with the increase of density of acid or base surface groups, as measured by potentiometric titration (Figure S2). Upon oxidation of the GNP-P, a 3-fold increase in the density of acidic groups was observed, from 0.20 nm^{-2} for GNP-P to 0.67 nm^{-2} for GNP-O (Figure 1, x-axis), which explains the low PZC. The GNP-N catalyst had only 0.22 nm^{-2} basic surface groups, possibly because of thermal decomposition of the O-containing groups under the harsh conditions ($T = 600\,°C$) of the ammonia treatment. GNP-H contained a negligible amount of acid-base surface groups, confirming their removal by the H_2-reduction treatment and therefore leading to a PZC close to 7.[26,32]

Figure 2 highlights the surface atomic composition, based on the XPS 1 s peaks of C, O and N elements, normalized by their sensitivity factor. The survey spectra (Figure S3) showed that C, O and N were indeed the only elements present. Therefore, the atomic surface compositions calculated can be directly compared to each other. The actual areas used in the calculation were not from the survey but from the high-resolution scans of N (Figure S4) and O (Figure S5). GNP-O showed a 2-times increase in the O content compared to the pristine material, with 8.7 at% and 4.1 at%, respectively (Table S1 and Figure 2a). This confirmed the successful introduction of O-containing groups upon oxidation treatment. The deconvolution of the O 1s peak revealed that GNP-O possessed the largest number of C–O (4.4 at%), C=O (3.5 at%) and COOH (0.8 at%) surface groups. Surprisingly, GNP-H presented an oxygen percentage (3.8 at%) similar to the pristine sample, suggesting that the difference in PZC is not directly related to the oxygen content but instead to the different chemical nature of the O-containing groups. GNP-H possessed 2.1 at% C–O and 1.3 at% C=O, while GNP-P showed 2.5 at% C–O and only 1.0 at% C=O. Furthermore, both catalysts had a small number of COOH groups, with only 0.2 at% for GNP-H and 0.4 at% for GNP-P. Although this difference is small and derived from a fitting model, it might explain the difference observed in PZC. The remarkably low amount of oxygen on GNP-N (0.7 at%) indicates that the ammonia treatment not only introduced N-containing groups, but also induced a thermal decomposition of the O-containing groups. Regarding the N content (Figure 2b), GNP-H, GNP-O and GNP-P presented a low N content (0.33 at%, 0.12 at% and 0.23 at%, respectively), only composed of pyrrolic groups. The difference in the N content of these catalysts is due to the reduction in the carbon surface area hence relative amount of C and O during the surface functionalization treatment. On the contrary, GNP-N carbon showed a wide range of N-groups, such as pyridinic (1.19 at%), pyrrolic (0.72 at%), graphitic nitrogen (0.21 at%), and pyridine N-oxide (0.12 at%).

Beside the surface groups analysis, the degree of graphitization, which influences the conductivity of the catalysts, was extrapolated from the XPS Auger peak.[34] All carbon catalysts showed around 77% of sp^2 carbon, demonstrating that the functionalization treatments did not affect the sp^2 character of the samples (Figure S6). To complete the characterization of the modified carbon materials, the X-ray diffraction patterns of the GNP-P, GNP-H, GNP-O and GNP-N catalysts were acquired and shown in the supporting information (Figure S7). The diffraction patterns of all surface-modified carbons were similar, meaning that the bulk graphitic structure was not significantly changed by the different surface modification treatments in line with earlier reports.[26] Representative scanning electron microscopy (SEM) images (Figure 3) of the freshly prepared electrodes show a uniform coverage of the carbon paper substrate with the modified carbon catalysts. The elemental analysis results showed only C, O and F, where the F came from the Nafion binder used to anchor the catalyst to the carbon paper. Furthermore, both EDX (Table S2) and XPS (Figure S3) did not show any metal impurity. They were also not expected in these samples, as the initial oxidation treatment was performed for all the catalysts in a highly concentrated nitric acid solution.

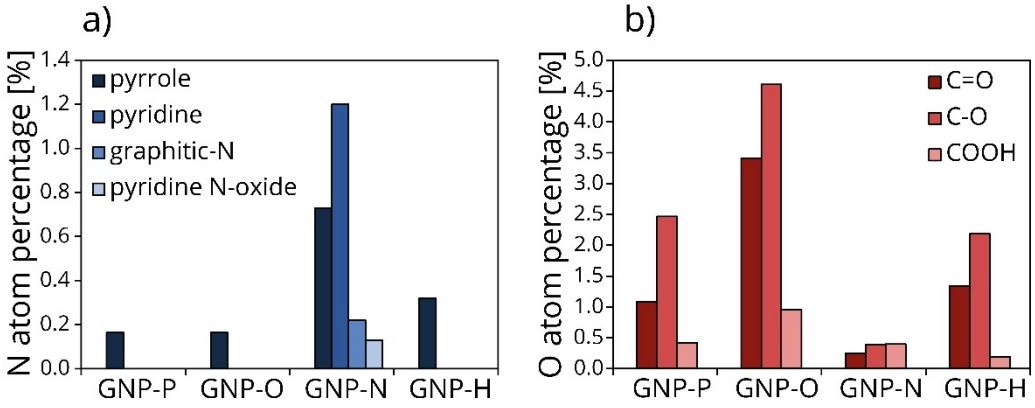

Figure 2. a) N-containing surface group quantification (atom percentage) based on XPS N 1s peak analysis and b) O-containing surface group quantification (atom percentage), where C=O and C–O at% is based on XPS O 1s peak analysis, while COOH at% is based on XPS C 1s peak analysis of the GNP-P, GNP-O, GNP-H and GNP-N electrocatalysts.

Research Article
doi.org/10.1002/ejic.202300152

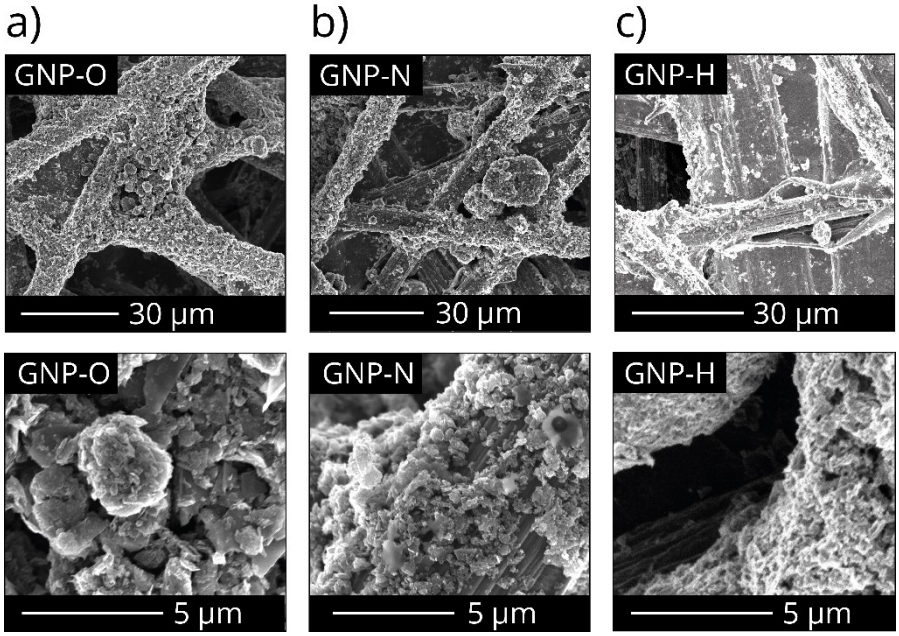

Figure 3. Representative SEM images of the surface-modified carbons a) GNP-O, b) GNP-N and c) GNP-H deposited on the carbon paper substrate. (Top) low magnification for an overview and (bottom) high magnification for a more detailed view.

Electrocatalytic reduction of CO_2

Figure 4 shows the total current density (j_{total}), normalized by the carbon surface area, as a function of the applied negative potential for GNP-H, GNP-O and GNP-N in a CO_2-saturated 0.1 M $KHCO_3$ aqueous solution at pH 6.8. The current density was obtained at four different potentials (−0.7, −0.9, −1.2 and −1.4 V vs RHE), averaging over 45 min. At −1.2 V vs RHE, GNP-H showed a current density of −20.1 mA m^{-2}, while GNP-O and GNP-N exhibited slightly larger current densities: −25.2 mA cm^{-2} and −28.2 mA cm^{-2} respectively. The different current densities can be explained by the difference in the catalytic activity of acid/base surface groups of which the GNP-O and GNP-N electrodes have a higher density than the GNP-H catalyst.[35–37]

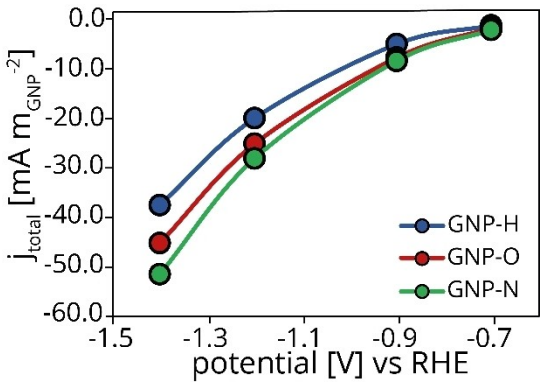

Figure 4. Total current density, as a function of the applied potential of GNP-H, GNP-O and GNP-N electrocatalyst in a CO2-saturated 0.1 M $KHCO_3$ electrolyte at pH 6.8.

To understand the influence of surface functionalization on the selectivity, we evaluated the CO and H_2 partial current densities, normalized to the carbon surface area. Figure 5a shows the hydrogen current densities as a function of the applied negative potential. The GNP-H catalyst gave the lowest current density with −18.9 mA m^{-2} at −1.2 V, while GNP-O and GNP-N produced a slightly larger H_2 current (−24.6 mA m^{-2} at −1.2 V vs RHE). This small current increase might be explained by an improved wetting of the carbon due the presence of polar surface groups on GNP-O and GNP-N.

Figure 5b shows the CO partial current densities of the modified catalysts. GNP-N is the only catalyst that shows a non-negligible CO current at only −0.9 V vs RHE. At −1.4 V vs RHE, GNP-N exhibits by far the largest CO current density, about 5.5 times higher than to the oxidized carbon and the reduced carbon. Furthermore, GNP-O produced formic acid, with a FE of 5.8% at only −0.7 V vs RHE (Table S3). The catalysts produced formic acid only at more cathodic potentials. As the precision in the quantification of formic acid via HPLC is limited,[3,7,12,20,24,38,39] we will mainly focused in the reminder of the paper, on understanding the selectivity towards CO.

In Figure 6, the CO Faraday efficiency (FE) for all the surface-modified carbons is shown as a function of the applied potential. At −0.7 V and −0.9 V vs RHE, GNP-H and GNP-O did not produce any CO. However, GNP-N produced 3.5% and 4.3% CO FE respectively, demonstrating that the CO_2 reduction began at lower overpotential. Upon increasing the potential to −1.2 V and −1.4 V vs RHE, the GNP-N electrocatalysts clearly produced most CO, with a FE of 5.1% and 8.6% respectively at these potentials. However, the FE is still dominated by the H_2 production at every potential (Figure S8).

Research Article
doi.org/10.1002/ejic.202300152

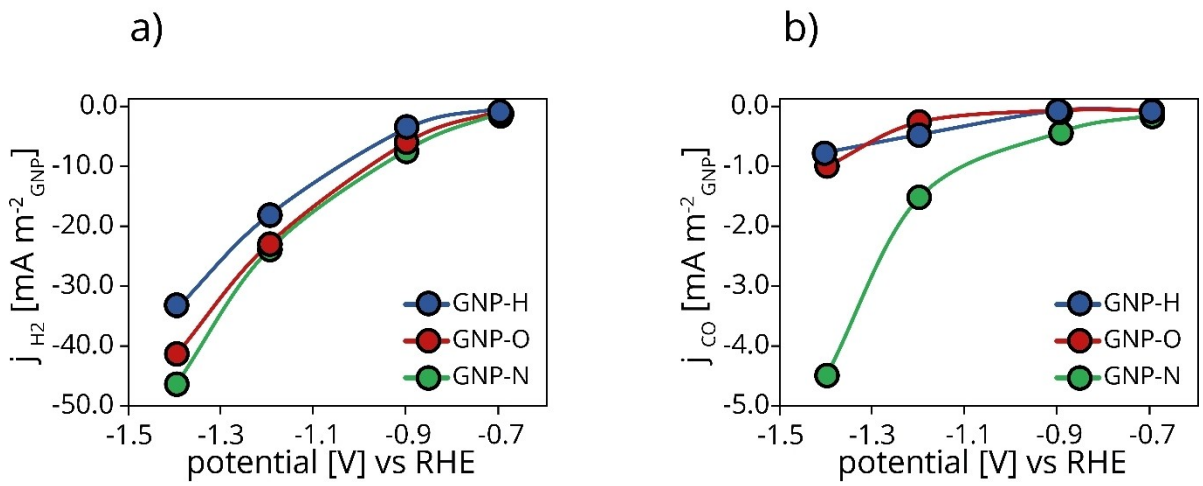

Figure 5. a) H_2 and b) CO partial current density normalized by carbon surface area, as a function of the applied potential of the GNP-H, GNP-O and GNP-N catalyst in a CO_2-saturated 0.1 M $KHCO_3$ electrolyte at pH 6.8.

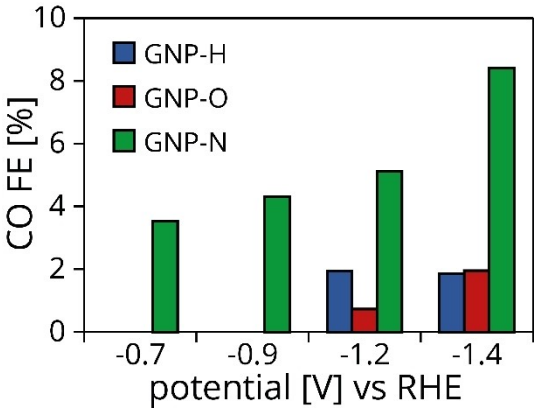

Figure 6. CO faradaic efficiency as a function of the applied potential, for the GNP-H, GNP-O and GNP-N catalyst in a CO_2-saturated 0.1 M $KHCO_3$ electrolyte at pH 6.8.

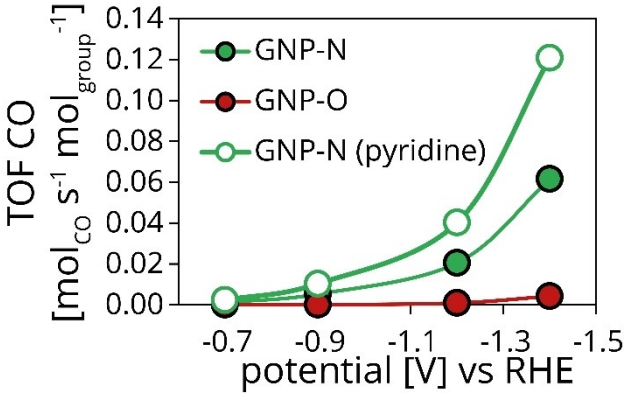

Figure 7. Turn over frequency (TOF) CO molar production per unit of time per mol surface group as a function of the applied potential. TOF was obtained through a combination of the CO partial current density and surface group analysis for GNP-N and GNP-O electrocatalyst. All the measurements were obtained in CO_2-saturated 0.1 M $KHCO_3$ 6.8 pH electrolyte.

Effect of the surface functional groups on the CO selectivity

To quantify the effect of different surface groups on the CO production, we calculated the CO turnover frequency (TOF) (Figure 7). This analysis is based on the assumption that the carbon surface (alone) is involved in H_2 evolution, while the functional surface groups are responsible for the CO evolution. The GNP-H catalyst was excluded from the analysis due to the uncertain nature of the active sites. Although the hydrogen treatment is meant to remove all surface groups, the process could have also introduced other type of defect on the carbon, but the nature of the defect is not yet well understood. Therefore, we attribute the activity of the GNP-H to the presence of such defects and/or to presence of low concentrations of the pyrrolic N groups (0.4 at%), after the hydrogen treatment.

At low overpotentials, the CO TOF of GNP-O (red marker) was negligible. In contrast, the TOF of GNP-N electrocatalyst (green marker) was 0.001 and 0.005 $mol_{CO}\,s^{-1}\,mol_{groups}{}^{-1}$ respectively. At −1.2 V and −1.4 V vs RHE, the N-containing groups showed a 15–20-fold higher intrinsic activity than the O-containing groups present on GNP-O catalyst. These results demonstrated that the structure and chemical properties of carbon surface groups plays a key role on the selective reduction of CO_2. By treating the carbon electrocatalysts, we modified their acidity/basicity. CO_2 is a weak Lewis acid,[40] and hence preferentially adsorbed and further converted on strong Lewis basic active sites. The XPS measurements (Figure 2) showed strong Lewis basic groups (pyridinic) on the surface of GNP-N (PZC = 9.1), which can explain its high CO partial current density. The lone electron pair on the pyridinic N atom can bind to the electrophilic C in CO_2, leading to *COOH formation, the first intermediate of the proton-coupled electron transfer pathway to CO.[19,41]

Although recent results from DFT calculations suggest that pyrrolic groups can contribute to CO formation at very high overpotentials, this has not been experimentally proven, rather most experimental evidence indicate that the pyridinic groups

Research Article
doi.org/10.1002/ejic.202300152

mostly determine the CO partial current density.[23] On the other hand, although the activity of the GNP-H which possess mainly very low concentration of pyrrolic groups suggests that this group might indeed be active towards CO_2RR, the exact nature of the defects in the GNP-H is not known, hence we only normalized the CO TOF to the pyridinic groups (Figure 7, empty markers) to avoid substantial errors.

Under this assumption, the intrinsic TOF of these groups is 0.12 $mol_{CO}\,s^{-1}\,mol_{pyridine}$ at −1.4 V vs RHE. Most of the published work on carbon-based electrocatalysts for CO_2 reduction involves materials produced via a bottom-up approaches, such as chemical-vapor deposition, using organic precursor such as pyridine, acetonitrile and dimthylformamide,[42] to achieve a high N content (in the carbon framework) and carefully designed graphene sheets. Hence, the selectivity and current density reported in literature is much higher, up to 80–85% CO FE and 100 $mA\,cm^{-2}$.[5,39,43] Interestingly, our work showed for the first time that simple surface functionalization procedure, starting from commercially available carbon powder, exhibits similar effects to a doping process. Furthermore, the combination of these simple procedures and a detailed surface characterization allowed to quantify the specific contribution of pyridinic groups to the CO TOF of GNP-N, giving a remarkable insight on the selectivity of these groups. Nevertheless, to confirm the correlation between selectivity descriptors and chemical nature of the surface groups, a large number of samples with different number of O- and N-containing groups needs to be synthesized and tested.

Although the specific CO TOF for carbon surface groups is not found in literature for this reaction, similar values were reported for more complex organometallic systems, such as carbon nanotubes functionalized with iron porphyrin (0.049 s^{-1}),[44] and nickel cyclam catalysts (0.015 s^{-1}),[45] tested in similar conditions.

Conclusions

A systematic study of the effect of surface-modification of graphitic carbon on its properties as electrode for the CO_2RR has been performed. Two different treatments introduced N-containing or O-containing surface groups, leading to basic or very acid surface properties. An alternative treatment removed surface groups, leading to a near neutral surface. The total current density, and the product selectivity of the CO_2 reduction were influenced by the nature and density of the surface groups. Especially the pyridinic groups showed a high intrinsic activity to form CO, while acidic groups rather led to formic acid production. Overall, the hydrogen evolution reaction on the carbon was still dominating, but our approach presented here showed for the first time that the selectivity can be rationally tuned by altering the surface chemistry via simple surface functionalization. By evaluating the CO turn over frequencies, it was found that nitrogen containing groups showed 20-times higher intrinsic selectivity compared to the oxygen containing groups.

Experimental Section

Chemicals

Graphitic carbon nanoplatelets XGnP500® (GNP) were purchased from XG Sciences, HNO_3 (65% wt/wt), sulfonated tetrafluoroethylene Nafion® 117 solution (5% in a mixture of lower aliphatic alcohols and water), isopropanol (99.5%) and potassium bicarbonate ($KHCO_3$, ≥99%) were purchased from Sigma Aldrich. A proton exchange Nafion™ N117 membrane was obtained from Ion Power, GmbH and carbon paper (TGP-H-060) was purchased from Toray.

Modification of the carbon materials

The modification of the graphitic carbon was performed by three different treatments. Surface oxidized carbon was obtained by liquid-phase oxidation using concentrated nitric acid.[27] Typically, 10 g of the as-received carbon material was suspended in 65% wt/wt HNO_3 (50 ml g_{carbon}^{-1}), inside a 1 l round bottom flask fitted with a reflux condenser. The suspension was heated to 80 °C, and kept at 80 °C for 120 min. Subsequently, the suspension was quenched by diluting it with deionized water. The solid carbon material sedimented on the bottom of the flask, and the supernatant was removed. The carbon material was washed rigorously with deionized water until the washing liquid reached a pH of around 7. Finally, the carbon powder was dried overnight at 120 °C. The surface-oxidized carbon is referred to as GNP-O. The final yield from the preparation of the GNP-O was 90%. This treatment was previously reported for the introduction of various oxygen-containing functional groups with a predominant surface coverage of carboxylic acid groups without having a significant change in the carbon crystal structure.[26,27,29,30,32,46] The reduced carbon (GNP-H) was obtained by treating oxidized GNP (0.3 g) in a flow of 20% H_2 and 80% Ar at a rate of 400 $mL\,min^{-1}$ at 400 °C for 12 h. The H_2 reduction treatment was meant to remove oxygen functional groups from the surface of the carbon (80% yield).[30,32] Amination treatment was performed with gaseous NH_3 at 600 °C at a flow rate of 0.25 $L\,min^{-1}$ per 0.3 g of carbon. This incorporates nitrogen-containing functional groups at the carbon surface[28,32,43,47] which in this work is referred to as GNP-N.

Working electrode preparation

The preparation of the working electrode was performed in three steps. First, a catalyst ink was prepared by mixing 11.8 mg modified carbon catalyst (sieve fraction <75 μm), 1120 μL isopropanol, 4470 μL MQ water and 44.4 μL Nafion solution. The ink was sonicated for 45 minutes in an ultrasonic bath to ensure a good dispersion of the catalyst powder in the Nafion containing solution. The resulting ink was sprayed onto a circular-shaped carbon paper substrate with a surface area of 4.9 cm^2 using an airbrush. Prior to the deposition of the catalyst, the carbon paper substrate was washed with ethanol under sonication for 30 minutes, and subsequently rinsed with milli-Q water. A catalyst loading of 0.2 mg/cm^2 was intended for all electrodes. The prepared electrodes were dried under vacuum overnight before each electrochemical testing.

Carbon characterization

To better understand the structure-selectivity relationship, we performed physical and chemical analyses on the modified carbon materials. The modified carbon catalysts were characterized using N_2-physisorption performed in a Micromeritics TriStar 3000 V6.08. Before the measurements, the carbon-based catalysts were dried at 170 °C under N_2-flow for 16 hours. The isotherms were measured at

Research Article
doi.org/10.1002/ejic.202300152

−196 °C using carbon black as a reference. The specific surface area was calculated using the multipoint Brunauer-Emmet-Teller (BET) method with p/p_0 between 0.05–0.25. The pore diameter was determined using the Barrett-Joyner-Halenda (BJH) method and the pore volume was determined as single point pore volume at $p/p_0 =$ 0.995.

SEM measurements of the surface-modified carbon on carbon paper were performed on the Phenom ProX from Thermo Fisher, operated at 10 kV. X-ray diffraction (XRD) measurements were done on a Bruker D2 Phaser, equipped with a Co Kα X-ray source with a wavelength of 1.79026 Å.

The point of zero charge of the carbon materials was measured by titration using a pH meter TitraLab. The amount of acidic and basic surface groups was determined in separate measurements. Typically, 25 mg of the modified carbon was suspended in 65 mL of 0.1 M KCl solution. The suspension was de-gassed with N_2 for 5 min under vigorous stirring. The titrations were performed using solutions of either 0.01 M NaOH or 0.01 M HCl, in 0.1 M KCl electrolyte. The acidic and basic groups densities were calculated from the titration curve showing the change in pH as a function of the volume of titrant. The inflection points on the curves were identified using the second derivative of the fitted curves. The inflection point corresponds to the titrant volume necessary to titrate the surface groups of the carbon, therefore at the inflection point, the moles of titrant are equal to the moles of surface groups on the carbon surface. This method is extensively used to measure the amount of surface groups present on materials surfaces.[27,32]

The XPS data were collected by using ThermoFischer Thermo Scientific K-Alpha X-ray Photoelectron Spectrometer System, with an Al source (Kα monochromatic radiation 1486.6 eV). The deconvolution of the carbon, oxygen and nitrogen peaks was performed by using CasaXPS. These measurements enable a better understanding of the influence of these surface groups on the activity and selectivity of the carbon material in the CO_2 reduction reaction.

Electrochemical measurements

The electrochemical measurements were performed in a custom-built H-type electrochemical cell with cathode and anode compartments separated by a Nafion membrane. 15 mL of 0.1 M $KHCO_3$ electrolyte at pH 7.5 was used in each compartment. The anolyte was constantly purged with argon and the catholyte was purged with CO_2 at 20 ml min^{-1}. The electrochemical measurements were performed with an Autolab PGSTAT204 Potentiostat, using a Pt disk as a counter electrode and a Ag/AgCl 3 M KCl reference electrode (Metrohm).

The modified-carbon catalysts deposited onto the carbon paper substrate were placed on a glassy carbon disk (3 cm diameter), which acted as an extra support for the carbon paper, and as the current collector. The glassy carbon and the carbon paper were held in place by O-shaped gaskets, leaving an electrode area of 3.8 cm^2 exposed to the electrolyte solution. The electrolyte was bubbled with CO_2 for 20 minutes before every electrocatalytic test, to achieve a homogeneous CO_2-saturation of the electrolyte, resulting in a pH of 6.8.

Chronoamperometry measurements for 45 minutes at different potentials were performed to determine the selectivity. The gaseous products were analyzed by an on-line gas chromatograph (Global Analysis Solutions Microcompact GC 4.0). The GC system was equipped with three channels. The first channel has an Rt-QBond (10 m*0.32 mm, Agilent) packed column and an FID detector for the detection of CH_4, C_2H_4 and C_2H_6, the second channel has a Molecular Sieve 5 A (10 m* 0.53 mm, Restek) packed column that separates small gaseous molecules such as CO and CH_4. This channel has an FID detector with a methanizer to increase the detection sensitivity of CO. The third channel has a Carboxen 1010 (8 m*0.32 mm, Agilent) packed column which separates H_2 and CO_2 with a TCD detector. High purity nitrogen (N_2; 99.999 %) was used as a carrier gas.

Liquid phase products were analyzed using a Varian HPLC equipped with a refractive index detector (RID) and a Bio-Rad Aminex HPX-87H column at 65 °C. 1 mM H_2SO_4 was used as the eluent with a flow rate of 0.55 mL min^{-1}. The retention time of formic acid was at 15 min and the total analysis time was 20 minutes.

The obtained potentials were converted to the reversible hydrogen electrode (RHE) potentials using equation 1:

$$\mathrm{E\ (vs.\ RHE)} = \mathrm{E\ (vs.\ Ag/AgCl)} + 0.209 + 0.059 \times \mathrm{pH} \quad (1)$$

The Faradaic efficiency for each modified carbon (FE) was calculated as shown in Equation (2):

$$FE(\%) = \frac{n_x\ x\ F\ x\ [moles\ of\ product\ x]}{Q} \times 100\,\% \quad (2)$$

In which n_x is the number of electrons needed to produce x product from CO_2 molecules and F is the Faradaic constant (96 485 s·A mol^{-1}).

For gaseous products ($x = H_2$, CO, and CH_4), the moles of the product were determined as shown in equation 3:

$$moles\ of\ product = \frac{C_X \times q \times p}{RT} \quad (3)$$

in which C_x is the volumetric concentration of product x in ppm extracted from the GC calibration plot, q is the gas flow rate, p is the pressure, R is the ideal gas constant (8.314 m^3 Pa K^{-1} mol^{-1}), T is the temperature, n_x is the number of reduced electrons needed to produce x (product) from CO_2 molecules and F is the Faradaic constant (96 485 s A mol^{-1}).

For liquid-phase products (x = formic acid), the moles of product formed were determined as shown in equation 4:

$$moles\ of\ product = \frac{C_X \times V_{catholyte}}{1000\ \times\ M_w} \quad (4)$$

in which C_x is the volumetric concentration of product x in ppm extracted from the HPLC calibration curve, $V_{catholyte}$ is the volume of the catholyte (L) and M_w the molar weight of product x (g mol^{-1}).

The turnover frequency (TOF), which corresponds to the intrinsic selectivity of the surface groups to CO, was calculated per mol of surface groups, using the following formula (equation 5):

$$TOF = \frac{j}{mol_{groups} * F * n} \quad (5)$$

Where j is the partial current of each individual product (CO), The total moles of surface groups (mol_{groups}) was calculated by multiplying the surface area of the carbon (m^2) by the density of surface groups (# m^{-2}) based on the theoretical weight of the surface-modified carbon over the carbon paper, finally the result is divided

by the Avogadro's number to obtain moles of surface groups (mol). *F* is the Faraday constant, and *n* is the number of electrons needed to produce the product of interest.

Acknowledgements

Francesco Mattarozzi was supported in collaboration with Shell Global Solutions International B. V. via the Advanced Research Center Chemical Building Blocks Consortium (ARC-CBBC). Marisol Tapia Rosales was supported by the NWO-EleReCet project, part of the Solar-to-Products program funded by the Dutch Research Council (NWO). Jan Willem de Rijk is acknowledged for useful discussions on the electrochemical set-up. Iris ten Have is acknowledged for the SEM images.

Conflict of Interests

The authors declare no conflict of interest.

Data Availability Statement

The data that support the findings of this study are available from the corresponding author upon reasonable request.

Keywords: Carbon materials · surface modification · CO_2 reduction reaction · electrochemistry · surface chemistry

[1] Y. Yang, S. Louisia, S. Yu, J. Jin, I. Roh, C. Chen, M. V. Fonseca Guzman, J. Feijóo, P. C. Chen, H. Wang, C. J. Pollock, X. Huang, Y. T. Shao, C. Wang, D. A. Muller, H. D. Abruña, P. Yang, *Nature* **2023**, *614*, 262–269.
[2] A. R. Woldu, P. Talebi, A. G. Yohannes, J. Xu, X. D. Wu, S. Siahrostami, L. Hu, X. C. Huang, *Angew. Chem. Int. Ed.* **2023**, *62*, e2023016.
[3] J. Wu, R. M. Yadav, M. Liu, P. P. Sharma, C. S. Tiwary, L. Ma, X. Zou, X. D. Zhou, B. I. Yakobson, J. Lou, P. M. Ajayan, *ACS Nano* **2015**, *9*, 5364–5371.
[4] S. Siahrostami, K. Jiang, M. Karamad, K. Chan, H. Wang, J. Nørskov, *ACS Sustainable Chem. Eng.* **2017**, *5*, 11080–11085.
[5] G. L. Chai, Z. X. Guo, *Chem. Sci.* **2016**, *7*, 1268–1275.
[6] Y. Sun, Q. Wu, G. Shi, *Energy Environ. Sci.* **2011**, *4*, 1113–1132.
[7] M. Pumera, *Energy Environ. Sci.* **2011**, *4*, 668–674.
[8] D. A. C. Brownson, D. K. Kampouris, C. E. Banks, *J. Power Sources* **2011**, *196*, 4873–4885.
[9] L. Dai, D. W. Chang, J.-B. Baek, W. Lu, *Small* **2012**, *8*, 1130–1166.
[10] H. Wang, X. Yuan, G. Zeng, Y. Wu, Y. Liu, Q. Jiang, S. Gu, *Adv. Colloid Interface Sci.* **2015**, *221*, 41–59.
[11] N. Yang, S. R. Waldvogel, X. Jiang, *ACS Appl. Mater. Interfaces* **2016**, *8*, 28357–28371.
[12] Z. Sun, T. Ma, H. Tao, Q. Fan, B. Han, *Chem* **2017**, *3*, 560–587.
[13] G. P. Hao, W. C. Li, D. Qian, G. H. Wang, W. P. Zhang, T. Zhang, A. Q. Wang, F. Schüth, H. J. Bongard, A. H. Lu, *J. Am. Chem. Soc.* **2011**, *133*, 11378–11388.
[14] P. Atkins, J. de Paula, in *Physical Chemistry*, W. H. Freeman, New York, **2006**.
[15] X. Sun, *Front. Chem.* **2021**, *9*, 1–9.
[16] A. S. Varela, W. Ju, A. Bagger, P. Franco, J. Rossmeisl, P. Strasser, *ACS Catal.* **2019**, *9*, 7270–7284.
[17] F. Pan, B. Li, W. Deng, Z. Du, Y. Gang, G. Wang, Y. Li, *Appl. Catal. B* **2019**, *252*, 240–249.
[18] X. Hao, X. An, A. M. Patil, P. Wang, X. Ma, X. Du, X. Hao, A. Abudula, G. Guan, *ACS Appl. Mater. Interfaces* **2021**, *13*, 3738–3747.
[19] M. Abdinejad, E. Irtem, A. Farzi, M. Sassenburg, S. Subramanian, H. P. Iglesias Van Montfort, D. Ripepi, M. Li, J. Middelkoop, A. Seifitokaldani, T. Burdyny, *ACS Catal.* **2022**, *12*, 7862–7876.
[20] J. Wu, S. Ma, J. Sun, J. I. Gold, C. Tiwary, B. Kim, L. Zhu, N. Chopra, I. N. Odeh, R. Vajtai, A. Z. Yu, R. Luo, J. Lou, G. Ding, P. J. A. Kenis, P. M. Ajayan, *Nat. Commun.* **2016**, *7*, 13869.
[21] R. Ma, K. Wang, C. Li, C. Wang, *Nanoscale Adv.* **2022**, *4*, 4197–4209.
[22] J. Yuan, W. Y. Zhi, L. Liu, M. P. Yang, H. Wang, J. X. Lu, *Electrochim. Acta* **2018**, *282*, 694–701.
[23] S. Liu, H. Yang, X. Huang, L. Liu, W. Cai, J. Gao, X. Li, T. Zhang, Y. Huang, B. Liu, *Adv. Funct. Mater.* **2018**, *28*, 1800499.
[24] F. Yang, X. Ma, W. Cai, P. Song, W. Xu, *J. Am. Chem. Soc.* **2019**, *51*, 20451–20459.
[25] M. P. van Heeswijk, J. H. Bitter, M. L. Toebes, A. J. van Dillen, K. P. de Jong, *Carbon* **2004**, *42*, 307–315.
[26] D. Sebastián, I. Suelves, R. Moliner, M. J. Lázaro, *Carbon* **2010**, *48*, 4421–4431.
[27] R. Beerthuis, J. W. de Rijk, J. M. S. Deeley, G. J. Sunley, K. P. de Jong, P. E. de Jongh, *J. Catal.* **2020**, *388*, 30–37.
[28] R. Arrigo, M. Hävecker, S. Wrabetz, R. Blume, M. Lerch, J. McGregor, E. P. J. Parrott, J. A. Zeitler, L. F. Gladden, A. Knop-Gericke, R. Schlögl, D. S. Su, *J. Am. Chem. Soc.* **2010**, *132*, 9616–9630.
[29] J. L. Figueiredo, *J. Mater. Chem. A* **2013**, *1*, 9351–9364.
[30] H. P. Boehm, *Carbon* **1994**, *32*, 759–769.
[31] J. L. Figueiredo, M. F. R. Pereira, *J. Energy Chem.* **2013**, *22*, 195–201.
[32] B. Donoeva, N. Masoud, P. E. De Jongh, *ACS Catal.* **2017**, *7*, 4581–4591.
[33] M. A. Montes-Morán, D. Suárez, J. A. Menéndez, E. Fuente, *Carbon* **2004**, *42*, 1219–1225.
[34] D. J. Morgan, *C* **2021**, *7*, 51.
[35] B. Buczek, S. Biniak, A. Światkowski, *Fuel* **1999**, *78*, 1443–1448.
[36] S. Mrozowski, *Carbon* **1971**, *9*, 97–109.
[37] K. H. Radeke, K. O. Backhaus, A. Swiatkowski, *Carbon* **1991**, *29*, 122–123.
[38] J. Wu, M. Liu, P. P. Sharma, R. M. Yadav, L. Ma, Y. Yang, X. Zou, X. Zhou, R. Vajtai, B. I. Yakobson, J. Lou, P. M. Ajayan, *Nano Lett.* **2016**, *16*, 466–470.
[39] H. Wang, Y. Chen, X. Hou, C. Ma, T. Tan, *Green Chem.* **2016**, *18*, 3250–3256.
[40] H. Kiuchi, R. Shibuya, T. Kondo, J. Nakamura, H. Niwa, J. Miyawaki, M. Kawai, M. Oshima, Y. Harada, *Nanoscale Res. Lett.* **2016**, *11*, 0–6.
[41] Y. Yan, E. L. Zeitler, J. Gu, Y. Hu, A. B. Bocarsly, *J. Am. Chem. Soc.* **2013**, *135*, 14020–14023.
[42] P. P. Sharma, J. Wu, R. M. Yadav, M. Liu, C. J. Wright, C. S. Tiwary, B. I. Yakobson, J. Lou, P. M. Ajayan, X. D. Zhou, *Angew. Chem. Int. Ed.* **2015**, *54*, 13701–13705.
[43] L. Chen, P. Peng, L. Lin, T. C. K. Yang, C. Huang, *Aerosol Air Qual. Res.* **2014**, *14*, 916–927.
[44] A. Maurin, M. Robert, *Chem. Commun.* **2016**, *52*, 12084–12087.
[45] F. Greenwell, G. Neri, V. Piercy, A. J. Cowan, *Electrochim. Acta* **2021**, *392*, 139015.
[46] B. M. Philippe Serp, in *Nanostructured Carbon Materials for Catalysis*, **2015**, pp. 20–33.
[47] M. G. Plaza, S. García, F. Rubiera, J. J. Pis, C. Pevida, *Sep. Purif. Technol.* **2011**, *80*, 96–104.

Manuscript received: March 26, 2023
Revised manuscript received: July 14, 2023
Accepted manuscript online: July 15, 2023
Version of record online: August 8, 2023